Synthetic physical interactions map kinetochore regulators and regions sensitive to constitutive Cdc14 localization

Guðjón Ólafsson and Peter H. Thorpe[1]

The Francis Crick Institute, Mill Hill Laboratory, London NW7 1AA, United Kingdom

Edited by Angelika Amon, Massachusetts Institute of Technology, Cambridge, MA, and approved July 17, 2015 (received for review March 31, 2015)

The location of proteins within eukaryotic cells is often critical for their function and relocation of proteins forms the mainstay of regulatory pathways. To assess the importance of protein location to cellular homeostasis, we have developed a methodology to systematically create binary physical interactions between a query protein and most other members of the proteome. This method allows us to rapidly assess which of the thousands of possible protein interactions modify a phenotype. As proof of principle we studied the kinetochore, a multiprotein assembly that links centromeres to the microtubules of the spindle during cell division. In budding yeast, the kinetochores from the 16 chromosomes cluster together to a single location within the nucleus. The many proteins that make up the kinetochore are regulated through ubiquitylation and phosphorylation. By systematically associating members of the proteome to the kinetochore, we determine which fusions affect its normal function. We identify a number of candidate kinetochore regulators, including the phosphatase Cdc14. We examine where within the kinetochore Cdc14 can act and show that the effect is limited to regions that correlate with known phosphorylation sites, demonstrating the importance of serine phospho-regulation for normal kinetochore homeostasis.

kinetochore | phosphatase | Mtw1 | MIND | CDK

The relocation of proteins between cellular compartments underlies many regulatory pathways. For example, protein relocation underpins most cell-signaling pathways (1) and the establishment of cell polarity and asymmetric cell division both require highly specialized relocation of proteins within the cell (2). Furthermore, the aberrant localization of proteins underlies the pathology of a number of diseases (3). However, our understanding of the effect of relocalizing members of the proteome is limited to specific studies typically concerning individual proteins, and only a select few studies have globally monitored protein relocation (4, 5).

One highly localized structure within the cell is the kinetochore, which in budding yeast forms a single megadalton complex (6–8). The kinetochore attaches chromosomes to the spindle microtubules to drive accurate chromosome segregation. The kinetochore consists of at least 60 unique gene products present in multiple copies that stretch from the specialized H3 histone subunit (Cse4, CENP-A in mammals) to the microtubule binding proteins of the Dam1 complex (9). Kinetochores normally assemble hierarchically from the centromere-bound proteins (10). Once assembled, the structural homeostasis of the kinetochore is regulated by proteins that are recruited to kinetochores. For example, the histone subunit Cse4 is tightly regulated by the E3 ubiquitin ligase Psh1, which is localized at centromeres. Psh1 prevents excessive Cse4 centromere loading via ubiquitylation-dependent degradation of Cse4 (and at non-centromeric regions) (11). Cse4 is also phosphorylated by Ipl1, likely to destabilize aberrant microtubule interactions and ensure correct sister chromosome biorientation (12). Another such modification is the phosphorylation and ubiquitylation of the MIND complex member Dsn1. Dsn1 is a target of both the cyclin-dependent kinase (CDK) and the Aurora kinase (Ipl1) (13, 14). Ipl1-dependent phosphorylation stabilizes Dsn1 and prevents its degradation by the Mub1/Ubr2 ubiquitin pathway. Additionally, the spindle assembly checkpoint, a key regulator of mitotic progression, is regulated via the selective, phospho-dependent, recruitment of proteins to the kinetochore (15–17). These data indicate that kinetochore homeostasis and mitotic control are regulated by posttranslational modifications and protein recruitment to the kinetochore.

To provide a map of kinetochore regulators, we wished to systematically recruit candidate proteins constitutively to the kinetochore and assay for a mitotic phenotype. To do this, we developed a system to artificially create protein–protein fusions across the proteome. We combined a GFP binding protein (18, 19) with a GFP library of strains (20) to create binary fusions between a kinetochore protein and most other proteins in the proteome. We used growth as a readout for kinetochore defects and any protein–protein interactions that affect growth we termed "synthetic physical interactions" or SPIs. We chose to study the kinetochore protein Mtw1, which is a conserved member of the MIND (Mis12) complex of the KMN (KNL1-Mis12-Ndc80) network of mid-/outer-kinetochore proteins (9). The SPI method identified proteins that, when bound to the kinetochore component Mtw1, cause a growth defect. For example, the Cdc14 phosphatase produces a SPI when bound to Mtw1. Cdc14 removes phosphates from CDK target sites, with a strong bias for phospho-serine over phospho-threonine (21). We then switched the GBP tag onto Cdc14 and used this to make fusions with GFP-tagged kinetochore proteins and show that the MIND complex, Dam1 complex, and COMA complex are all sensitive to constitutive Cdc14 binding. Thus, we created a map of regions

Significance

The localization of proteins within the cell is assumed to be important for their function. However, we have limited understanding of protein relocalization in response to genetic changes or drug treatments and almost no understanding of the effects of protein relocation on cellular homeostasis. To address this, we have developed a method to systematically create protein fusions between a query protein and most other proteins in the cell. As proof of principle, we relocalized proteins to the kinetochore, a large protein complex essential for chromosome segregation and cell division. We identify a number of proteins that inhibit cell division via the kinetochore. One such interaction establishes a critical role for specific phosphorylation in kinetochore function.

Author contributions: G.Ó. and P.H.T. designed research, performed research, analyzed data, and wrote the paper.

The authors declare no conflict of interest.

This article is a PNAS Direct Submission.

[1]To whom correspondence should be addressed. Email: Peter.Thorpe@crick.ac.uk.

This article contains supporting information online at www.pnas.org/lookup/suppl/doi:10.1073/pnas.1506101112/-/DCSupplemental.

within the kinetochore that are sensitive to constitutive Cdc14 phosphatase activity. In some cases these phosphorylation events have been mapped (22, 23) and studied in some detail (14); however, the role of Cdc14 in kinetochore function remains unclear (24, 25). This study establishes that phosphorylation of proteins at the kinetochore is essential for normal mitotic progression in yeast. The SPI methodology identifies specific protein–protein interactions that control a given phenotype and thus provides a powerful tool to study the spatial regulation of proteins at a systems level.

Results

To identify regulators of kinetochore homeostasis we wanted to systematically and constitutively recruit specific proteins to the kinetochore. To achieve this aim, we made use of an antibody domain that binds with high affinity to GFP (18, 19), the GFP binding protein (GBP). We chose to study Mtw1, the yeast ortholog of human Mis12. Mtw1 is a member of the essential Mtw1/Mis12/MIND complex (Mtw1, Dsn1, Nnf1, and Nsl1) (26, 27). The MIND complex connects the inner constitutive centromere-associated network kinetochore proteins, which are adjacent to the centromeric DNA, with the outer, microtubule-associated proteins in conjunction with Mif2 (28–31). We linked the *MTW1* kinetochore gene with that of the *GBP* (*MTW1-GBP*). By virtue of the RFP tag on the GBP, we can identify the Mtw1-GBP in live cells and confirm that it localizes with the kinetochore. A plasmid encoding Mtw1-GBP can be transferred into a library of GFP strains to allow us to sequentially fuse a GBP-tagged protein with an array of GFP-tagged proteins (Fig. 1*A* and Fig. S1*A*). We were readily able to delete the endogenous *MTW1* gene from a strain containing the *MTW1-GBP* plasmid, indicating that the fusion is functional. We created two other constructs to control for the effects of both expressing *MTW1* ectopically and for the nonspecific effects of GBP binding to GFP-tagged proteins. These controls were used as the basis for comparison with the *MTW1-GBP*. We confirmed that the GBP colocalizes in vivo to GFP-tagged proteins (Fig. 1 *B–D*). We expressed *MTW1-GBP* in cells encoding proteins tagged with CFP, to which the GBP does not bind, and found that this tagged version of Mtw1 colocalizes with the kinetochore (Fig. 1 *E–G*). Furthermore, we found that the Mtw1-GBP is sufficient to constitutively relocalize GFP-tagged proteins to the kinetochore (Fig. 1 *H–J*).

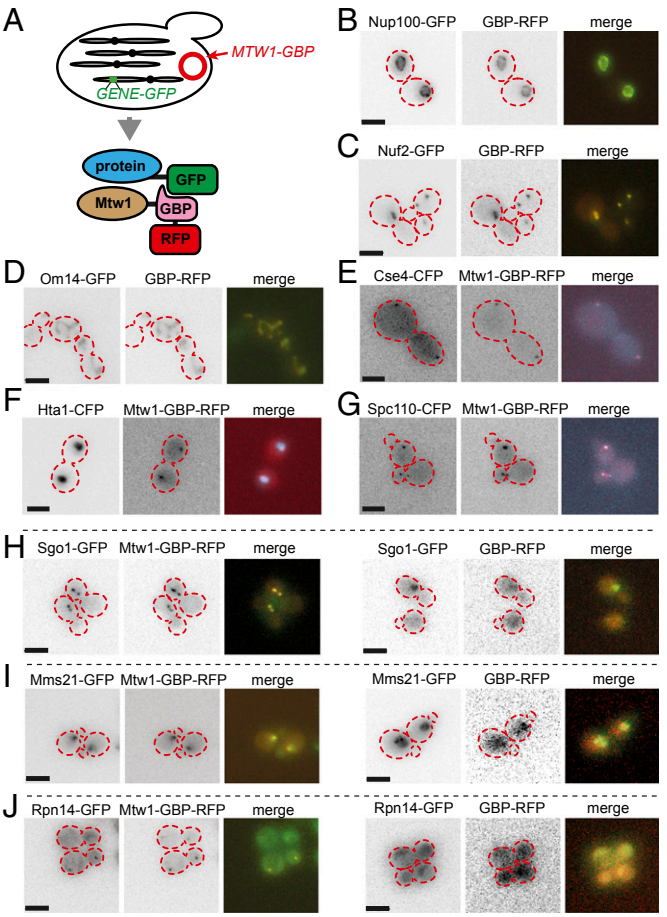

Fig. 1. (*A*) The SPA methodology introduces a plasmid encoding, for example Mtw1-GBP (red circle) into an array of GFP strains. The Mtw1 query protein is fused with the GFP binding protein and also contains an RFP sequence to allow us to monitor its location. The GBP-RFP is efficiently recruited to GFP-tagged proteins in different cellular compartments in vivo, such as the nuclear pore (*B*, Nup100), the kinetochore (*C*, Nuf2), or the mitochondria (*D*, Om14). The Mtw1-GBP protein localizes to the kinetochore in the nucleus of yeast cells as indicated by its position relative to the kinetochore (*E*), nucleus (*F*), and spindle pole body (*G*). Mtw1-GBP colocalizes with three GFP-tagged proteins, which normally do not localize with Mtw1 (*H–J*). The three panels on the right show the normal localization of these proteins and the three panels on the left show their localization when bound to Mtw1. The GFP tagged proteins with GBP-RFP localize as previously reported [yeastgfp.yeastgenome.org (20)]. The cell boundaries are overlaid as red dashed lines. (Scale bars, 5 μm.)

Proteome-Wide Kinetochore Fusions. We transferred the *MTW1-GBP* plasmid and, separately, the two controls, *MTW1* and *GBP*, into the GFP collection of strains using selective ploidy ablation (SPA) (32) (Fig. S1*A*), which produces arrays of haploid GFP-tagged strains, each containing one of the three plasmid constructs. The relative growth of the resulting strains was assessed by colony size, measured in quadruplicate for each strain, and quantified using the ScreenMill suite of software (33) (*SI Text*). An example of these data illustrates that specific GFP strains are restricted for growth with Mtw1-GBP compared with either of the two controls (Fig. 2*A*). Comparing the growth rate of strains expressing *MTW1-GBP* with either the *MTW1* or the *GBP* control yielded well-correlated data for strains demonstrating a growth defect (Fig. S1 *B* and *C*), therefore we used the average growth relative to the two controls as a measure of growth effects (Fig. 2*B*). For these proteome-wide data, growth defects were quantified and then normalized using *z*-score. High *z*-scores indicate a growth defect produced by the Mtw1-GBP interaction with the GFP-tagged protein. Most forced interactions have no discernable growth effect upon the cells (*z*-score ~0). Relative to the two controls, 128 GFP strains had a growth defect defined by an average *z*-score ≥ 1.5 (Dataset S1). We defined interactions that affect growth as SPIs. A number of these SPI proteins have essential functions in the cell and, although we controlled for nonspecific protein interactions, we wished to know how many of these interactions result from the relocalization of an essential GFP protein. We reasoned that these interactions would be suppressed by having an untagged version of the GFP-tagged protein present in the cell. Therefore, we modified the proteome-wide screen, retaining the cells as diploids that are heterozygously GFP-tagged (Fig. 2*C* and Fig. S1*A*). We assayed these diploid strains for growth, as previously described. The resulting growth rates (Fig. 2*D*) showed that 56 strains were inhibited from growth (*z*-score > 1.5) (Dataset S2), of which the majority (34 strains) were common with the haploid set of SPIs (Fig. 2*D*, *Inset*).

SPIs Share Common Functions. Because functionally related genes and proteins are enriched for interactions (genetic, physical, and so forth) (34, 35), we asked whether the Mtw1 SPIs were enriched for interactions from genomics and proteomics databases. We used the Cutoff Linked to Interaction Knowledge tool (CLIK) (36) to plot the interaction density of the haploid and

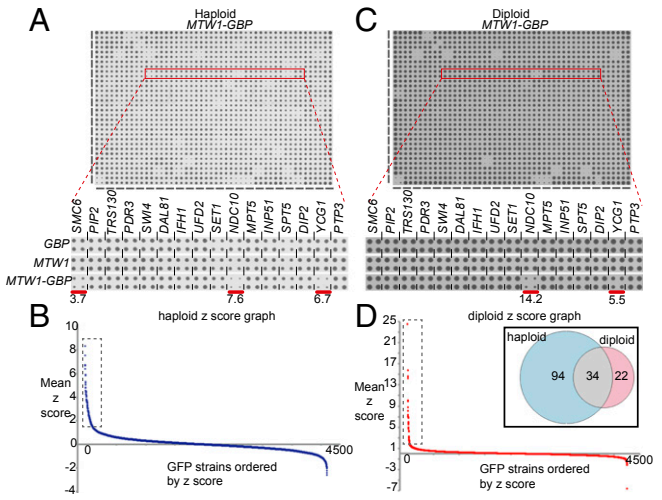

Fig. 2. Mtw1 synthetic physical interactions. (*A*) An example of 384 yeast GFP strains each arrayed in quadruplicate. The *MTW1-GBP* construct is expressed in these strains and the growth of colonies on the plate are shown. (*Inset*) An example of 16 strains from the plate, three of which show growth restriction compared with the two controls (*GBP* and *MTW1*). The red bars indicate the three growth-restricted strains, with the *z*-score indicated. (*B*) Quantitation of the colony size allows us to calculate *z*-scores for each interaction (higher score indicates greater growth restriction). The strains are ranked based upon their *z*-score, with the most growth-restricted strains to the left. Only a relatively small subset of interactions affect growth; 128 strains have an average *z*-score greater than 1.5 (boxed group, full data in Dataset S1). (*C*) The same assay was repeated in heterozygously tagged diploid strains, where for each strain there is an untagged allele in addition to the GFP-tagged version. (*Inset*) The same 16 strains highlighted in *A*. (*D*) Quantitative analysis of the diploid screen shows that 56 strains are significantly restricted for growth (boxed group and Dataset S2). The inset Venn diagram indicating that a majority of the diploid SPIs (34 of 56) are common with those from the haploid screen.

diploid SPI screens (Fig. S1 *D* and *E*, respectively). The CLIK plot shows that both the haploid and diploid screens enrich for a set of ~100 SPIs that have a high interaction density (i.e., are likely true positives). To assess the false discovery rate (FDR) and to corroborate the CLIK analysis we retested the haploid and diploid screens with the interactions that caused the strongest growth defects with 16 replicates. This high-density retest of the SPIs identified 112 haploid and 79 diploid SPIs (Datasets S3 and S4; for an example, see Fig. S1*F*). Of the original 34 SPIs that were common between haploid and diploid screens, only one failed to confirm; additionally, the high-density retest confirmed a number of additional SPIs. As a result, 61 Mtw1 SPIs are common between the haploid and diploid sets after high-density retesting. These data show that the SPI data are reproducible with good correlation of the proteome-wide *z*-scores with the high-density repeated data (Fig. S1 *G* and *H*). We also found that, as expected for quantitative screens, the FDR increased as the strength of the phenotype decreased (Fig. S1 *I* and *J*). Additionally, the number of confirmed SPIs was in good agreement with that predicted by the CLIK analysis. Finally, we asked whether SPIs correlate with protein abundance, because low-abundance proteins may be more susceptible to disruption simply based upon stoichiometric interaction with Mtw1-GBP, but we found no correlation (Fig. S1 *K* and *L*).

Collectively these data show that the SPI methodology is robust and identifies a set of proteins that are enriched for genetic and physical interactions, indicating that they share common functionality. To test this notion, we used gene ontology enrichment analysis (37) within the set of 61 confirmed SPIs, which when constitutively bound to the kinetochore result in a growth defect. These Mtw1 SPIs are significantly enriched for a number of different functional classes or protein complexes, including chromosome organization, histone modification/deacetylation, nuclear transport, the nuclear pore, and condensin (Fig. S2). This enrichment is illustrated for a subset of confirmed SPIs (Fig. 3). Furthermore, phenotype enrichment analysis (38) shows that mutants of the genes encoding the Mtw1 SPIs give both a chromosomal instability (CIN) phenotype and show synthetic lethality with proteins involved in sumoylation (Fig. S3). These data indicate that the Mtw1 SPIs are enriched for proteins that likely play an important role in kinetochore function. To ask whether CIN was associated with the SPI phenotype, we used an established assay for CIN (39) in diploid cells that encode a single GFP allele and contain the plasmid-encoded Mtw1-GBP. We found that of five Mtw1 SPIs tested, three show a clear CIN phenotype (Cdc5, Tom70, and Ypr174c) (Fig. S4 *A* and *B*). To test whether these SPI phenotypes were caused by association with the kinetochore or by movement of the kinetochore to a new location within the nucleus, we used fluorescence imaging. We found that Mtw1-GBP is sufficient to relocalize both Cdc5-GFP and Ypr174c-GFP to the kinetochore (Fig. S5 *A* and *B*, respectively). In contrast, the nucleoporin Nup1, when associated with Mtw1, moves the tagged version of Mtw1 into close association with the nuclear periphery without relocalizing the kinetochore structure itself (Fig. S5*C*). Association between the mitochondrial translocase Tom70 and Mtw1 leads to abnormal kinetochore foci (Fig. S5*D*). These imaging studies support the notion that the Mtw1-GBP recruits proteins to the kinetochore that are not tightly bound structural components (such as Cdc5); however, proteins such as Nup1 and Tom70, which are tightly bound to defined structural complexes, do not relocalize. We cannot rule out that relocation of some Mtw1 from the kinetochore does not, at least partially, contribute to the SPI phenotype. The GFP–GBP interaction itself is strong (19) and this creates a molecular "tug-of-war" between the two tagged proteins.

SPI Analysis Identifies a Role for Kinetochore Phosphorylation. Three of the 61 Mtw1 SPIs are directly involved in phospho-regulation. First, Dbf4 is the regulatory subunit of the Cdc7 kinase. Second, the

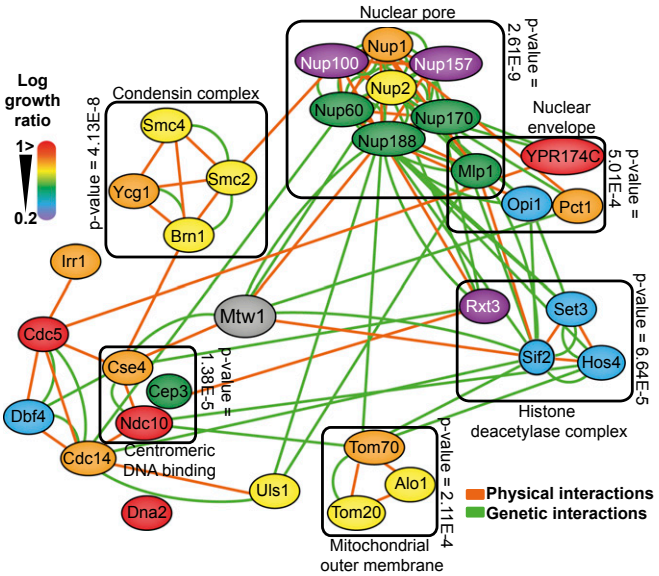

Fig. 3. Mtw1 SPI network. A subset of the confirmed Mtw1 SPIs (a group of 31 SPIs that were common between haploid and diploids in both the proteome-wide analysis and also the high-density retest) are shown as nodes, color coded according to the strength of the SPI (red indicates strong interactions, purple indicates weak interactions). The enriched genetic and physical interactions between these proteins are indicated by green and orange edges, respectively. A selection of the gene ontology enrichment for this set of proteins is indicated by grouping related proteins in boxes with the associated *P* value of enrichment.

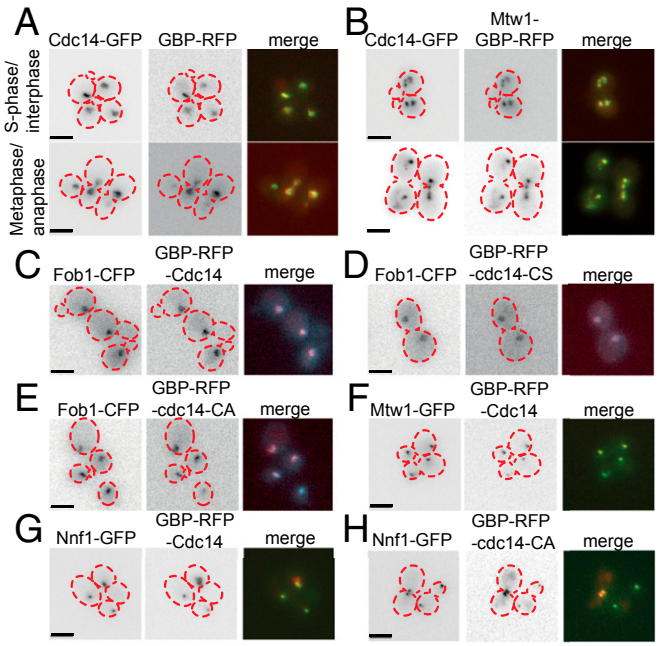

Fig. 4. The Mtw1-Cdc14 SPI is the result of Cdc14 recruitment to kinetochores. (*A*) Cdc14 is normally localized to the nucleolus and when tagged with GFP can recruit GBP. (*B*) Mtw1-GBP recruits Cdc14-GFP to the kinetochores, and this results in mitotic defects, such as lagging kinetochores. (*C–E*) GBP-Cdc14 and the catalytically inactive variants are normally localized to the nucleolus, as shown by colocalization with nucleolar protein Fob1. Inclusion of a GFP-tagged kinetochore protein, such as Mtw1-GFP or Nnf1-GFP, is sufficient to recruit either GBP-Cdc14 (*F* and *G*) or phosphatase-dead GBP-Cdc14-C283A (*H*) to the kinetochore. Cell outlines are indicated with red dashed lines. (Scale bars, 5 μm.)

polo-like kinase Cdc5 was identified as a high-copy suppressor of *DBF4* mutants (40). Finally, Cdc14 is a mitotic phosphatase that reverses the effects of the CDK to facilitate the progression from mitosis to G_1. We focused upon Cdc14, a conserved phosphatase that is released from the nucleolus during anaphase to act upon CDK targets principally within the nucleus (21, 41). Cdc14 normally localizes to kinetochores during late mitosis and is important for targeting the chromosomal passenger complex to kinetochores (42). To determine the effect of the Mtw1-Cdc14 SPI in live cells, we used imaging and genetic analysis. We found that cells containing both Mtw1-GBP and Cdc14-GFP have constitutive association of Cdc14 and Mtw1 and aberrant kinetochore foci are observed in these cells (Fig. 4 *A* and *B*). We found that association of Cdc14 with Mtw1 caused an increase in large-budded cells (Fig. S4*C*), although without leading to a CIN phenotype (Fig. S4 *A* and *B*). This Mtw1-Cdc14 SPI phenotype could be caused by recruitment of Cdc14 to the kinetochore, by association of the entire kinetochore into the nucleolus or by impairing kinetochore assembly by titrating away Mtw1-bound proteins. We examined the location of the kinetochore, Cdc14, and the nucleolus using fluorescence imaging. We found that Cdc14 is relocalized to kinetochores (Fig. S5 *E* and *F*), although we noted that some Mtw1 was relocalized to the nucleolus. To evaluate this Mtw1-Cdc14 SPI in more detail and to examine the role of Cdc14 at the kinetochore, we used the SPI system to recruit Cdc14 to different kinetochore proteins, essentially performing the reciprocal fusion to that identified in the proteome-wide screen. We created constructs that encode Cdc14 alone, GBP-Cdc14 (both N- and C-terminal fusions), and mutants of *CDC14* that encode catalytically inactive phosphatases (N-terminally tagged) GBP-Cdc14-CA and GBP-Cdc14-CS and also (C-terminally tagged) Cdc14-CA-GBP. Cdc14 tagged with GBP localized normally to the nucleolus (Fig. 4 *C–E*). The *CDC14-GBP-RFP* allele can be introduced into the endogenous *CDC14* locus, indicating it functions normally within the cell (Table S1). We transferred these constructs separately into a set of 88 kinetochore and kinetochore-related GFP strains (Dataset S5) using the SPA methodology, with 16 replicates. Thus, we constitutively associated Cdc14 with each complex within the kinetochore structure and evaluated its effect. The GBP-tagged versions of Cdc14 (both wild-type and mutant) were recruited to GFP-tagged kinetochores (Fig. 4 *F–H*). We next compared the growth of Cdc14-GBP with both untagged Cdc14 and with either of the catalytic-dead mutants, which allowed us to query the effect of the phosphatase activity. A number of strains are inhibited for growth specifically by the catalytically active form of the Cdc14 phosphatase (Fig. 5 *A* and *B* and Fig. S6*A*). We quantified the growth effects as previously described (33), comparing the wild-type GBP-Cdc14 with either Cdc14 or the catalytically inactive mutants. The two N-terminally tagged mutants (*GBP-cdc14-CA* and *GBP-cdc14-CS*) gave equivalent results (Fig. S6*B* and Dataset S5). Additionally, the data for the N- and C-terminally tagged versions of Cdc14 were well correlated (Fig. S6*C*). Regardless of which GBP-Cdc14 construct is used or which control was compared, we found that members of the MIND complex consistently cause a growth defect (Fig. 5 *A* and *B* and Fig. S6*A*). In addition to individual SPIs from other complexes, there is evidence to support a growth defect for Cdc14 association with members of the outer kinetochore Dam1 complex (Dad1, Dad2, and Dad3), the inner kinetochore Cbf3 complex (Ndc10 and Cep3), and the COMA complex (Mcm21 and Ctf19).

To determine whether the stoichiometry of Cdc14-GBP is a determinant of the SPI phenotype, we compared the fluorescence from endogenously tagged Cdc14-GBP-RFP with that of plasmid-encoded Cdc14-GBP-RFP (either wild-type or mutant). The plasmid creates ~150% of the normal level of Cdc14 protein (Fig. S7*A*). We then correlated the Cdc14 SPIs with protein abundance and found no correlation (Fig. S7 *B* and *C*). We also

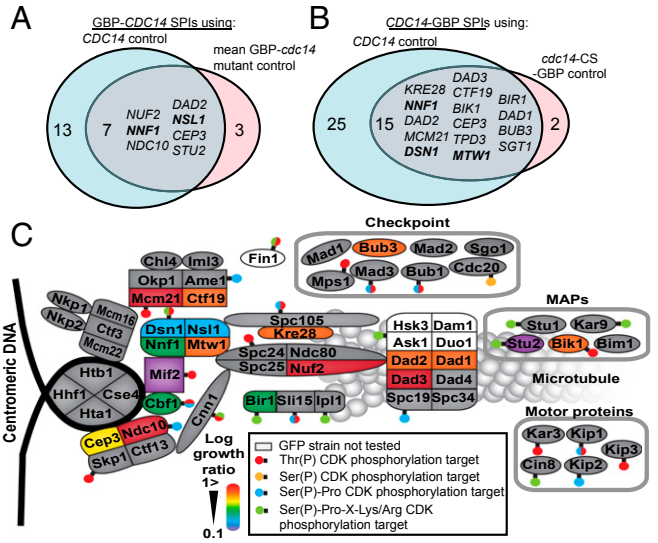

Fig. 5. Cdc14 recruitment only affects a subset of kinetochore proteins. (*A*) The N-terminally tagged Cdc14 compared with Cdc14 gave SPI phenotypes with 20 GFP strains and compared with the catalytically inactive mutant gave 10 SPIs, 7 of which overlap between the two groups (Dataset S5). (*B*) The C-terminally tagged Cdc14 gave 40 SPIs relative to the Cdc14 control and 17 relative to a catalytically inactive mutant, of which 15 overlap (Dataset S5). Members of the MIND complex are identified in both screens. (*C*) Cdc14-kinetochore SPIs overlap with known phosphorylation sites. A schematic of the kinetochore shows many of the key kinetochore proteins, each of which is color-coded: red indicates the Cdc14 SPIs with the strongest growth defects and purple the weakest; gray proteins were not identified as SPIs in this assay. Superimposed upon this schematic as "lollipops" are the previously mapped CDK sites within the kinetochore.

used increasing copper concentrations to up-regulate the levels of plasmid-encoded Cdc14 (Fig. S7*D*) and found that higher levels of Cdc14 have only minor effects upon SPI phenotype (Fig. S7 *E–H* and Dataset S5).

To ask whether the Cdc14-kinetochore SPIs require checkpoint activation, we created a set of 22 GFP strains that are deleted for *MAD3*, a critical downstream component of the spindle assembly checkpoint. We repeated the SPI screen with both wild-type GFP-tagged strains and *mad3Δ* versions of each of these. The SPI phenotypes were not suppressed by deletion of *MAD3*, indicating that checkpoint is not necessary for the Cdc14 SPI phenotype (Fig. S6 *E* and *F* and Dataset S5). Some of the Cdc14 interactions give a slightly stronger growth defect in *mad3Δ* strains (e.g., Nsl1, Ame1, or Cep3), indicating that these SPIs create problems for the kinetochore, which are normally suppressed by an active checkpoint. We also repeated the screen in the presence of benomyl and this did not significantly affect any of the SPIs (Dataset S5). We also marked a region of chromosome five (at the *URA3* locus) with a repressor–operator system and found that the Mtw1–Cdc14 interaction does not exclusively arrest cells before metaphase (Fig. S4*D*). These data indicate that the mitotic checkpoint is not directly producing the SPI phenotype, nor do the SPIs result in checkpoint deficiency.

Dsn1 Dephosphorylation Does Not Cause the SPI Phenotype. Dsn1 is the only member of the MIND complex known to contain CDK target sites (22, 23), but blocking phosphorylation of these sites does not result in significant mitotic phenotypes (13). To ask whether association of Cdc14 adjacent to the MIND complex could affect phosphorylation of Dsn1, we tagged endogenous Dsn1 with the sequence encoding three HA tags. We found that Dsn1 phosphorylation is reduced upon recruitment of wild-type Cdc14 to the MIND complex in comparison with mutant Cdc14 (Fig. S6*D*), although CDK dephosphorylation of Dsn1 is not lethal; therefore, we could not link the SPI phenotype allele with this particular dephosphorylation event. It is possible that by constitutively recruiting Cdc14 adjacent to Dsn1, the two non-CDK serines (S240 and 250) are dephosphorylated. Ipl1-dependent phosphorylation of these two serines stabilizes Dsn1 and prevents its ubiquitin-mediated degradation by Ubr2 and Mub1 (14). However, the SPI phenotype of the MIND complex with Cdc14 is not rescued in a *ubr2Δ* strain (Fig. S8*A*), nor are the Cdc14 SPIs with Nnf1, Nsl1, or Nuf2 (Fig. S8*B*). Additionally, we created a set of new GBP constructs from the kinetochore (Nuf2, Mif2, and Ctf19) and tested their effect in a *CDC14-GFP* strain. These fusions all give SPI phenotypes in both wild-type *UBR2* and *ubr2Δ* cells (Fig. S8*C*). Hence, deletion of *UBR2* fails to rescue the growth defect of Cdc14 with the MIND complex. To test this in another way, we created a plasmid construct expressing a mutant form of *DSN1*, in which the codons for serines 240 and 250 are converted to those of aspartic acid (S240,250D). This construct would therefore create a pool of stabilized Dsn1 that cannot be degraded in the canonical Ubr2-dependent way (14). This *DSN1 S240,250D* plasmid was used in a Cdc14 SPI assay of the kinetochore and the original SPI phenotype (with members of the MIND complex) is not rescued by inclusion of this stabilized Dsn1 construct (Fig. S9). We also performed the same experiment with other Dsn1 variants, first with the canonical CDK site changed to aspartic acid (S264D), second with a Dsn1 variant that included changes to two other proposed CDK sites (S69,170,264D), and third with all of these serines changed to aspartic acid (S69,170,240,250,264D). In no case did the mutations of *DSN1* rescue the SPI phenotype of recruiting Cdc14 to the MIND complex (Fig. S9). Thus, we conclude that dephosphorylation of CDK and Ipl1 sites within Dsn1 is not responsible for the SPI phenotype.

Irrespective of the CDK or other phosphorylation sites, these data indicate that phosphorylation of proteins at the kinetochore is important for normal mitotic function. The Cdc14 fusions that cause SPIs are superimposed upon a graphic of the kinetochore structure (Fig. 5*C*) to produce a map of these Cdc14 phosphatase-sensitive regions within the yeast kinetochore.

Discussion

Key steps in kinetochore assembly and homeostasis are regulated by specific posttranslational modifications, such as phosphorylation and ubiquitylation (9). We have developed a proteome-wide approach to systematically query which protein–protein interactions affect kinetochore homeostasis. We identified a small subset of these forced interactions that significantly affect growth and termed these synthetic physical interactions. SPIs define pairs of proteins that when forced together affect the growth of the cells. Mutations in the genes encoding Mtw1 SPIs give a CIN phenotype and have synthetic interactions with sumoylation mutants. Recently, a number of kinetochore proteins have been identified that are sumoylated (43). Among the Mtw1 SPIs are a number of proteins that associate with the inner kinetochore, including Rfa1, Brn1, Nmd5, and Cdc5 (11). The latter of these, Cdc5, is the polo-like kinase, which regulates the dynamic association between kinetochores and microtubules (44). More generally, phosphorylation plays an important role in kinetochore homeostasis and we noted that one Mtw1 SPI was with Cdc14. CDK phosphorylates a number of kinetochore proteins and Cdc14, when released from the nucleolus in anaphase, reverses a number of these phosphorylations (22, 23, 42, 45). However, the importance of these CDK phosphorylation/dephosphorylation events is unclear. For example, Dsn1 is a member of the MIND complex, which is dephosphorylated before the bulk release of Cdc14 (13). However, *CDC14* conditional mutants only have a subtle defect in mitosis (25). To map the effects of Cdc14 phosphatase activity, we used the SPI method to recruit both wild-type and inactive variants of Cdc14 to different kinetochore proteins. We found that a number of kinetochore complexes are sensitive to constitutive recruitment of the active phosphatase, including the MIND complex, the Cbf3 complex, and the Dam1 complex. Although it is possible that the Mtw1-Cdc14 SPI phenotype is caused by partial relocation of Mtw1 to another location (e.g., the nucleolus), this is unlikely for a number of reasons. First, the mutant Cdc14 binding causes equal kinetochore relocation as the wild-type (Fig. 4 *G* and *H*), but does not give a SPI phenotype. Second, we did not identify other Cdc14-associated nucleolar proteins in the original Mtw1 SPI screen, despite screening most of the proteome. Third, not all kinetochore proteins produce a SPI phenotype with Cdc14. Fourth, our stoichiometry analysis does not support sequestration of low-abundance kinetochore proteins away from the kinetochore (Fig. S7 *B* and *C*). Finally, these Cdc14 SPIs correlate well with a map of the CDK sites within the kinetochore (Fig. 5*C*). We show that although phosphorylation of Dsn1 is inhibited by recruitment of Cdc14, this dephosphorylation is unlikely to result in the Cdc14-Mtw1 SPI. Therefore, we speculate that either the Cdc14 is removing other phosphates in neighboring proteins—for example, CDK serine sites on Cnn1 (24), Sli15 (42), Bir1 (46), or Fin1 (47) (Fig. 5*C*)—or at non-CDK sites on other proteins. In any of these cases, the Cdc14 SPIs highlight the importance of phosphorylation of kinetochore proteins for mitosis and warrant further characterization of the role of phosphorylation in regulating kinetochore homeostasis. Because Cdc14 normally functions as a dimer, the catalytically inactive mutants may be capable of recruiting wild-type Cdc14 to the kinetochore (48, 49). This would produce false-negatives in our screen; hence, it is possible that our list of sites affected by Cdc14 is an underrepresentation of all of the critical CDK sites at the kinetochore. Another approach would be to recruit CDK or other kinases to the kinetochore to determine whether constitutive phosphorylation would also affect

mitosis. Such a fusion method is highly effective in specific cases (50, 51).

Collectively, these data show that the SPI methodology is sufficiently robust to create protein fusions across the proteome. Furthermore, we show proof of principle that the SPI methodology identifies functional interactions in a similar way to synthetic genetic interactions. A spatial map of serine-phosphatase–sensitive sites within the kinetochore correlates well with existing CDK data, strongly supporting a role for functional CDK phosphorylation in mitotic kinetochore function. The SPI methodology is adaptable for use with either entire proteins or functional domains and has broad application for exploring the role of protein localization at a systems level.

Experimental Procedures

The yeast strains used in this study are listed in Table S1. Strains were constructed using standard techniques and standard yeast growth medium including 2% (wt/vol) of the indicated carbon source (52). Yeast plasmids are listed in Table S2. Plasmids were transferred into the GFP strains using selective ploidy ablation (32) and the resulting colony growth assessed using ScreenMill software (33). Other methods are described in *SI Text*.

ACKNOWLEDGMENTS. We thank Helen Caulston, Dana Pe'er, Grant Brown, Ulrich Rothbauer, Henrich Leonhardt, Rodney Rothstein, Bob Reid, John Dittmar, Frank Uhlmann, Meghna Kataria, and Lisa Berry for reagents, comments on this manuscript, and other help. Singer Instruments provided assistance with high-throughput yeast genomics. This work was funded by the Medical Research Council (MC_UP_A252_1027). The Francis Crick Institute is funded by Cancer Research UK, the Medical Research Council, and the Wellcome Trust.

1. Scott JD, Pawson T (2009) Cell signaling in space and time: Where proteins come together and when they're apart. *Science* 326(5957):1220–1224.
2. Nelson WJ (2003) Adaptation of core mechanisms to generate cell polarity. *Nature* 422(6933):766–774.
3. Hung MC, Link W (2011) Protein localization in disease and therapy. *J Cell Sci* 124(Pt 20):3381–3392.
4. Tkach JM, et al. (2012) Dissecting DNA damage response pathways by analysing protein localization and abundance changes during DNA replication stress. *Nat Cell Biol* 14(9):966–976.
5. Handfield LF, Chong YT, Simmons J, Andrews BJ, Moses AM (2013) Unsupervised clustering of subcellular protein expression patterns in high-throughput microscopy images reveals protein complexes and functional relationships between proteins. *PLOS Comput Biol* 9(6):e1003085.
6. Goshima G, Yanagida M (2000) Establishing biorientation occurs with precocious separation of the sister kinetochores, but not the arms, in the early spindle of budding yeast. *Cell* 100(6):619–633.
7. He X, Asthana S, Sorger PK (2000) Transient sister chromatid separation and elastic deformation of chromosomes during mitosis in budding yeast. *Cell* 101(7):763–775.
8. Pearson CG, Maddox PS, Salmon ED, Bloom K (2001) Budding yeast chromosome structure and dynamics during mitosis. *J Cell Biol* 152(6):1255–1266.
9. Biggins S (2013) The composition, functions, and regulation of the budding yeast kinetochore. *Genetics* 194(4):817–846.
10. Collins KA, Castillo AR, Tatsutani SY, Biggins S (2005) De novo kinetochore assembly requires the centromeric histone H3 variant. *Mol Biol Cell* 16(12):5649–5660.
11. Ranjitkar P, et al. (2010) An E3 ubiquitin ligase prevents ectopic localization of the centromeric histone H3 variant via the centromere targeting domain. *Mol Cell* 40(3):455–464.
12. Boeckmann L, et al. (2013) Phosphorylation of centromeric histone H3 variant regulates chromosome segregation in *Saccharomyces cerevisiae*. *Mol Biol Cell* 24(12): 2034–2044.
13. Akiyoshi B, Biggins S (2010) Cdc14-dependent dephosphorylation of a kinetochore protein prior to anaphase in *Saccharomyces cerevisiae*. *Genetics* 186(4):1487–1491.
14. Akiyoshi B, et al. (2013) The Mub1/Ubr2 ubiquitin ligase complex regulates the conserved Dsn1 kinetochore protein. *PLoS Genet* 9(2):e1003216.
15. Musacchio A, Salmon ED (2007) The spindle-assembly checkpoint in space and time. *Nat Rev Mol Cell Biol* 8(5):379–393.
16. London N, Biggins S (2014) Mad1 kinetochore recruitment by Mps1-mediated phosphorylation of Bub1 signals the spindle checkpoint. *Genes Dev* 28(2):140–152.
17. Yamagishi Y, Yang CH, Tanno Y, Watanabe Y (2012) MPS1/Mph1 phosphorylates the kinetochore protein KNL1/Spc7 to recruit SAC components. *Nat Cell Biol* 14(7):746–752.
18. Rothbauer U, et al. (2008) A versatile nanotrap for biochemical and functional studies with fluorescent fusion proteins. *Mol Cell Proteomics* 7(2):282–289.
19. Rothbauer U, et al. (2006) Targeting and tracing antigens in live cells with fluorescent nanobodies. *Nat Methods* 3(11):887–889.
20. Huh WK, et al. (2003) Global analysis of protein localization in budding yeast. *Nature* 425(6959):686–691.
21. Bremmer SC, et al. (2012) Cdc14 phosphatases preferentially dephosphorylate a subset of cyclin-dependent kinase (Cdk) sites containing phosphoserine. *J Biol Chem* 287(3):1662–1669.
22. Ubersax JA, et al. (2003) Targets of the cyclin-dependent kinase Cdk1. *Nature* 425(6960):859–864.
23. Holt LJ, et al. (2009) Global analysis of Cdk1 substrate phosphorylation sites provides insights into evolution. *Science* 325(5948):1682–1686.
24. Malvezzi F, et al. (2013) A structural basis for kinetochore recruitment of the Ndc80 complex via two distinct centromere receptors. *EMBO J* 32(3):409–423.
25. D'Amours D, Stegmeier F, Amon A (2004) Cdc14 and condensin control the dissolution of cohesin-independent chromosome linkages at repeated DNA. *Cell* 117(4):455–469.
26. De Wulf P, McAinsh AD, Sorger PK (2003) Hierarchical assembly of the budding yeast kinetochore from multiple subcomplexes. *Genes Dev* 17(23):2902–2921.
27. Cheeseman IM, Chappie JS, Wilson-Kubalek EM, Desai A (2006) The conserved KMN network constitutes the core microtubule-binding site of the kinetochore. *Cell* 127(5):983–997.
28. Przewloka MR, et al. (2011) CENP-C is a structural platform for kinetochore assembly. *Curr Biol* 21(5):399–405.
29. Screpanti E, et al. (2011) Direct binding of Cenp-C to the Mis12 complex joins the inner and outer kinetochore. *Curr Biol* 21(5):391–398.
30. Petrovic A, et al. (2010) The MIS12 complex is a protein interaction hub for outer kinetochore assembly. *J Cell Biol* 190(5):835–852.
31. Kline SL, Cheeseman IM, Hori T, Fukagawa T, Desai A (2006) The human Mis12 complex is required for kinetochore assembly and proper chromosome segregation. *J Cell Biol* 173(1):9–17.
32. Reid RJ, et al. (2011) Selective ploidy ablation, a high-throughput plasmid transfer protocol, identifies new genes affecting topoisomerase I-induced DNA damage. *Genome Res* 21(3):477–486.
33. Dittmar JC, Reid RJ, Rothstein R (2010) ScreenMill: A freely available software suite for growth measurement, analysis and visualization of high-throughput screen data. *BMC Bioinformatics* 11:353.
34. Novick P, Osmond BC, Botstein D (1989) Suppressors of yeast actin mutations. *Genetics* 121(4):659–674.
35. Gavin AC, et al. (2002) Functional organization of the yeast proteome by systematic analysis of protein complexes. *Nature* 415(6868):141–147.
36. Dittmar JC, Pierce S, Rothstein R, Reid RJ (2013) Physical and genetic-interaction density reveals functional organization and informs significance cutoffs in genome-wide screens. *Proc Natl Acad Sci USA* 110(18):7389–7394.
37. Eden E, Navon R, Steinfeld I, Lipson D, Yakhini Z (2009) GOrilla: A tool for discovery and visualization of enriched GO terms in ranked gene lists. *BMC Bioinformatics* 10:48.
38. Thorpe PH, Dittmar JC, Rothstein R (2012) ScreenTroll: A searchable database to compare genome-wide yeast screens. *Database (Oxford)* 2012:bas022.
39. Yuen KW, et al. (2007) Systematic genome instability screens in yeast and their potential relevance to cancer. *Proc Natl Acad Sci USA* 104(10):3925–3930.
40. Kitada K, Johnson AL, Johnston LH, Sugino A (1993) A multicopy suppressor gene of the *Saccharomyces cerevisiae* G1 cell cycle mutant gene dbf4 encodes a protein kinase and is identified as *CDC5*. *Mol Cell Biol* 13(7):4445–4457.
41. Queralt E, Uhlmann F (2008) Cdk-counteracting phosphatases unlock mitotic exit. *Curr Opin Cell Biol* 20(6):661–668.
42. Pereira G, Schiebel E (2003) Separase regulates INCENP-Aurora B anaphase spindle function through Cdc14. *Science* 302(5653):2120–2124.
43. Yong-Gonzales V, Hang LE, Castellucci F, Branzei D, Zhao X (2012) The Smc5-Smc6 complex regulates recombination at centromeric regions and affects kinetochore protein sumoylation during normal growth. *PLoS One* 7(12):e51540.
44. Liu D, Davydenko O, Lampson MA (2012) Polo-like kinase-1 regulates kinetochore-microtubule dynamics and spindle checkpoint silencing. *J Cell Biol* 198(4):491–499.
45. Kao L, et al. (2014) Global analysis of cdc14 dephosphorylation sites reveals essential regulatory role in mitosis and cytokinesis. *Mol Cell Proteomics* 13(2):594–605.
46. Widlund PO, et al. (2006) Phosphorylation of the chromosomal passenger protein Bir1 is required for localization of Ndc10 to the spindle during anaphase and full spindle elongation. *Mol Biol Cell* 17(3):1065–1074.
47. Akiyoshi B, Nelson CR, Ranish JA, Biggins S (2009) Quantitative proteomic analysis of purified yeast kinetochores identifies a PP1 regulatory subunit. *Genes Dev* 23(24):2887–2899.
48. Taylor GS, Liu Y, Baskerville C, Charbonneau H (1997) The activity of Cdc14p, an oligomeric dual specificity protein phosphatase from *Saccharomyces cerevisiae*, is required for cell cycle progression. *J Biol Chem* 272(38):24054–24063.
49. Gray CH, Good VM, Tonks NK, Barford D (2003) The structure of the cell cycle protein Cdc14 reveals a proline-directed protein phosphatase. *EMBO J* 22(14):3524–3535.
50. Lyons NA, Morgan DO (2011) Cdk1-dependent destruction of Eco1 prevents cohesion establishment after S phase. *Mol Cell* 42(3):378–389.
51. Coudreuse D, Nurse P (2010) Driving the cell cycle with a minimal CDK control network. *Nature* 468(7327):1074–1079.
52. Sherman F (2002) Getting started with yeast. *Methods Enzymol* 350:3–41.
53. Baryshnikova A, et al. (2010) Quantitative analysis of fitness and genetic interactions in yeast on a genome scale. *Nat Methods* 7(12):1017–1024.
54. Collins SR, Schuldiner M, Krogan NJ, Weissman JS (2006) A strategy for extracting and analyzing large-scale quantitative epistatic interaction data. *Genome Biol* 7(7):R63.
55. Keogh MC, et al. (2006) A phosphatase complex that dephosphorylates gammaH2AX regulates DNA damage checkpoint recovery. *Nature* 439(7075):497–501.
56. Thomas BJ, Rothstein R (1989) The genetic control of direct-repeat recombination in *Saccharomyces*: The effect of *rad52* and *rad1* on mitotic recombination at *GAL10*, a transcriptionally regulated gene. *Genetics* 123(4):725–738.
57. Zou H, Rothstein R (1997) Holliday junctions accumulate in replication mutants via a RecA homolog-independent mechanism. *Cell* 90(1):87–96.